ResearchGate

See discussions, stats, and author profiles for this publication at: https://www.researchgate.net/publication/8187928

Inhibition of Islet Amyloid Polypeptide Fibril Formation: A Potential Role for Heteroaromatic Interactions †

ARTICLE *in* BIOCHEMISTRY · DECEMBER 2004

Impact Factor: 3.02 · DOI: 10.1021/bi048582a · Source: PubMed

CITATIONS
136

READS
76

4 AUTHORS, INCLUDING:

Yariv Mazor
MedImmune, LLC
16 PUBLICATIONS **647** CITATIONS
SEE PROFILE

Shimon Efrat
Tel Aviv University
91 PUBLICATIONS **4,530** CITATIONS
SEE PROFILE

Ehud Gazit
Tel Aviv University
176 PUBLICATIONS **8,913** CITATIONS
SEE PROFILE

Available from: Yariv Mazor
Retrieved on: 01 February 2016

Inhibition of Islet Amyloid Polypeptide Fibril Formation: A Potential Role for Heteroaromatic Interactions†

Yair Porat,‡ Yariv Mazor,‡ Shimon Efrat,§ and Ehud Gazit*,‡

Department of Molecular Microbiology and Biotechnology, Tel Aviv University, Tel Aviv 69978, Israel, and Department of Human Genetics and Molecular Medicine, Sackler School of Medicine, Tel Aviv University, Tel Aviv 69978, Israel

Received July 5, 2004; Revised Manuscript Received September 5, 2004

ABSTRACT: The formation of amyloid fibril is associated with major human diseases, including Alzheimer's disease, prion diseases, and type 2 diabetes. Methods for efficient inhibition of amyloid fibril formation are therefore highly clinically important. A principal approach for the inhibition of amyloid formation is based on the use of modified molecular recognition elements. Here, we demonstrate efficient inhibition of amyloid formation of the type 2 diabetes-related human islet amyloid polypeptide (hIAPP) by a modified aromatic peptide fragment and a small aromatic polyphenol molecule. A molecular recognition assay using peptide array analysis suggested that molecular recognition between hIAPP and its core amyloidogenic module is mediated by aromatic rather than hydrophobic interactions. To study the possible effect of aromatic interactions on inhibition of hIAPP fibril formation, we have used peptide and small molecule inhibitors. The addition of a nonamyloidogenic peptide analogue of the core module NFGAILSS, in which phenylalanine was substituted with tyrosine (NYGAILSS), resulted in substantial inhibition of fibril formation by hIAPP. The inhibition was significantly stronger than the one achieved using a β-sheet breaker-conjugated peptide NFGAILPP. On the basis of the molecular arrangement of the tyrosine−phenylalanine interaction, we suggest that the inhibition stems from the geometrical constrains of the heteroaromatic benzene−phenol interaction. In line with this notion, we demonstrate remarkable inhibition of hIAPP fibril formation and cytotoxicity toward pancreatic β-cells by a small polyphenol molecule, the nontoxic phenol red compound. Taken together, our results provide further experimental support for the potential role of aromatic interactions in amyloid formation and establish a novel approach for its inhibition.

The formation of amyloid fibrils is associated with a large group of diseases of unrelated origin, including Alzheimer's disease, prion diseases, and type 2 diabetes (*1*, *2*). Pancreatic amyloid deposits composed of the human islet amyloid polypeptide (hIAPP)[1] are found in more than 90% of type 2 diabetes patients, and their toxicity is assumed to be an important factor in pancreatic β-cell failure in late stages of the disease (*3*, *4*). The hIAPP hormone, which is cosecreted with insulin, forms amyloid fibrils *in vitro* that are cytotoxic to β-cells (*5*). These fibrils, or most likely their protofibrillar forms, are assumed to play a key role in the diabetic process by the cytotoxic destruction of β-cells (*6*−*8*). Inhibition of amyloid fibril formation is therefore considered a key prospect therapeutic approach toward diabetes and other amyloid-related diseases (*9*−*17*).

A small fragment of hIAPP, the $hIAPP_{22-29}$ (NFGAILSS) octapeptide core module, forms fibrils that are similar to those formed by the full-length polypeptide (*18*, *19*). We demonstrated the essential role of the phenylalanine residue in the formation of amyloid fibrils by this fragment by an alanine scan (*20*). We have also shown that substitution of the phenylalanine residue with tyrosine in the context of the NYGAILSS octapeptide has reduced dramatically its amyloidogenic potential to form fibrils (*21*). On the basis of the above, other experimental observations on the role of aromatic residues in amyloidogenic polypeptides (*21*−*24*), and the well-known role of aromatic stacking in processes of self-assembly in chemistry and biochemistry (*25*−*28*), it was suggested that stacking of aromatic residues may play a role in the acceleration of the assembly process in many cases of amyloid fibril formation (*20*, *23*, *24*). Stacking interactions may provide an energetic contribution as well as directionality and orientation that are facilitated by the restricted geometry of planar aromatic rings stacking. We further demonstrated that short aromatic dipeptides contain all the molecular information to self-assemble into well-ordered nanostructures that are structurally related to amyloid fibrils (*29*).

Here, we use our mechanistic insights into the process of hIAPP amyloid formation to devise a novel approach of inhibition using heteroaromatic interactions. An octapeptide

† This work was supported by TAU Future Technology LP (to E.G.).

* To whom correspondence should be addressed: Department of Molecular Microbiology and Biotechnology, Tel Aviv University, Tel Aviv 69978, Israel. E-mail: ehudg@post.tau.ac.il. Telephone: +972-3-640-9030. Fax: +972-3-640-9407.

‡ Department of Molecular Microbiology and Biotechnology.

§ Department of Human Genetics and Molecular Medicine, Sackler School of Medicine.

[1] Abbreviations: hIAPP, human islet amyloid polypeptide; MBP, maltose binding protein; CD, circular dichroism; DMSO, dimethyl sulfoxide; HFIP, 3,3,3,3′,3′,3′-hexafluoro-2-propanol; PR, phenol red; SEM, scanning electron microscopy; TEM, transmission electron microscopy.

10.1021/bi048582a CCC: $27.50 © 2004 American Chemical Society
Published on Web 10/19/2004

fragment of hIAPP, with one aromatic substitution of phenylalanine with tyrosine, and a polyphenol small molecule (phenol red) are shown to inhibit hIAPP fibril formation. Furthermore, we show that phenol red can be used as a nontoxic inhibitor of β-cell cytotoxicity.

EXPERIMENTAL PROCEDURES

Peptide Synthesis and Preparation of Stock Solutions. Peptide synthesis using solid-phase methods was performed by Peptron Inc. (Taejeon, Korea) for $hIAPP_{22-29}$ peptide analogues and by Calbiochem for $hIAPP_{1-37}$. The correct identity of the peptides was confirmed by ion spray mass spectrometry, and the purity of the peptides was confirmed by reverse phase high-pressure liquid chromatography. $hIAPP_{22-29}$ stock solutions were prepared by dissolving the lyophilized form of the peptides in Me_2SO (DMSO) at a concentration of 100 mM. The stock solution for $hIAPP_{1-37}$ was prepared by dissolving the lyophilized form of the peptide in 3,3,3,3′,3′,3′-hexafluoro-2-propanol (HFIP) at a concentration of 400 μM. To avoid any preaggregation, all stock solutions were sonicated for 2 min before each experiment. MALDI-TOF mass spectrometry analysis (using an Applied Biosystems Voyager DE-STR spectrometer) revealed that no fragmentation of the polypeptide occurred after sonication.

MBP−IAPP Fusion Protein Expression and Purification. This protocol is based on previous work (*30*). Briefly, for expression of IAPP fused to the C-terminus of MBP, *Escherichia coli* cells transformed with expression plasmid pMALc2x-IAPP were grown in 200 mL of LB medium supplemented with 100 μg/mL ampicillin and 1% (w/v) glucose and induced with 0.5 mM IPTG. Cell extracts were prepared in 10 mM phosphate buffer (pH 7.5) and protease inhibitor cocktail (Sigma-Aldrich), by freezing and thawing followed by a brief sonication. The extracts were clarified by centrifugation at 20000*g* and stored at 4 °C. MBP−IAPP fusion protein was purified by passing the extract over an amylose resin column (New England Biolabs) and recovered by elution with 20 mM maltose in 20 mM Tris-HCl (pH 7.4), 1 mM EDTA, 200 mM NaCl buffer.

Membrane Binding Assay. An array of 19 synthetic decamers that contain the core $hIAPP_{20-29}$ amyloidogenic fragment (SNNFGAILSS), with all possible natural amino acid substitutions (except cysteine) at the position of phenylalanine 23 (Jerini), was used. Following blocking with 5% (v/v) nonfat milk in 25 mM Tris-buffered saline (TBS, pH 7.4), the membrane was incubated in the presence of 25 μg/mL MBP−hIAPP at 4 °C for 12 h. The membrane was then washed repeatedly with 0.05% (v/v) Tween 20 in TBS. Interaction of the MBP−IAPP fusion protein (or MBP as a control) with the membrane-bound peptides was detected with an anti-MBP monoclonal antibody (Sigma) and a HRP-conjugated goat anti-mouse secondary antibody. An immunoblot was developed using liquid 3,3′-diaminobenzidine.

Kinetic Aggregation Assay. The $hIAPP_{22-29}$ peptide stock solution was diluted into 10 mM Tris-HCl (pH 7.2) buffer to a final concentration of 1 mM peptide and 4% DMSO. Turbidity was measured at 405 nm at room temperature using disposable UVette cuvettes (Eppendorf) using a Scinco S-3100 spectrophotometer.

Thioflavin T Fluorescence Assay. A stock solution of synthetic $hIAPP_{1-37}$ was diluted to a final concentration of 4 μM in 10 mM sodium acetate buffer (pH 6.5) with or without inhibitor (40 μM), and a final HFIP concentration of 1% (v/v). Immediately after dilution, the sample was centrifuged at 4 °C for 20 min at 20000*g*, and the supernatant was used for fluorescence measurements. ThT was added to a final concentration of 3 μM, and fluorescence was measured using a Perkin-Elmer 50SB fluorimeter (excitation at 450 nm, 2.5 nm slit; emission at 482 nm, 10 nm slit). For the phenol red inhibition, samples were diluted 10-fold so that the maximal phenol red concentration did not exceed 4 μM, and measured using a Jobin Yvon Horiba Fluoromax 3 fluorimeter (excitation at 450 nm, 2.5 nm slit; emission at 482 nm, 5 nm slit).

Circular Dichroism Spectroscopy. hIAPP (4 μM) was prepared as described above, with or without inhibitor (40 μM). Spectra were recorded at 25 °C with 1 nm intervals and an averaging time of 4 s, using an AVIV 202 CD spectrometer. Final scan values represent subtraction of the baseline (buffer in the case of hIAPP and buffer with inhibitor for the inhibition assay). The overall contribution of the inhibitors was relatively minor. The spectra of the inhibitors in buffer are available as Supporting Information.

Transmission Electron Microscopy. Samples (10 μL) of $hIAPP_{22-29}$ from the aggregation assay and hIAPP from the fluorescence assay were placed on 400 mesh copper grids (SPI Supplies, West Chester, PA) covered by carbon-stabilized Formvar film. After 1 min, excess fluid was removed, and the grids were negatively stained with 2% uranyl acetate in water for 2 min. Samples were viewed in a JEOL 1200EX electron microscope operating at 80 kV.

MTT Reduction Assay. βTC-tet cells (*31*) or PC12 cells were plated in 24-well plates (2×10^5 cells/well) or 96-well plates (1×10^4 cells/well), respectively, and allowed to adhere for 24 h. A synthetic hIAPP stock solution was diluted to a final concentration of 4 μM in serum free growth medium (*31*) containing DMEM with or without phenol red. Immediately after dilution, samples were centrifuged at 4 °C for 20 min at 20000*g*, and the supernatant was bubbled with nitrogen for 30 min to evaporate residual HFIP. Cells were washed twice with PBS and incubated with the supernatant for 24 h. MTT was then added for 3 h, followed by addition of lysis buffer and incubation overnight. Samples were read at 570 nm. Cell viability was calculated in comparison to that of cells incubated in the absence of hIAPP, in medium with or without phenol red.

Scanning Electron Microscopy. Cells were grown on glass microscope cover slips under the same conditions as for the MTT assay. Immediately after incubation with hIAPP, the cells were fixed with 2% glutaraldehyde (v/v) and stored for 24 h at 4 °C. The cells were serially dehydrated with increasing concentrations of ethanol (30, 50, 70, 90, 95, and 100%) and dried with a critical point drier. Specimen cover slips were coated with colloidal gold and viewed using a JEOL JSM 840A microscope operating at 25 kV.

RESULTS

Profound understanding of the molecular mechanism that leads to amyloid fibril self-assembly is a key factor in the ability to design efficient inhibitors of the self-assembly process. Our previous studies on the role of phenylalanine 23 in fibril formation by hIAPP have led us to focus on the

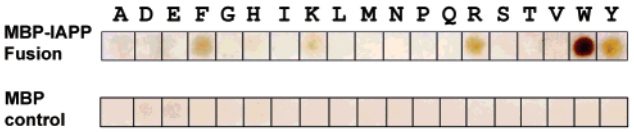

FIGURE 1: Molecular recognition of $hIAPP_{20-29}$ peptide analogues by $hIAPP_{1-37}$. A synthetic peptide array containing analogues of $hIAPP_{20-29}$ (SNN**F**GAILSS) with all the possible natural amino acid substitutions (except cysteine) at the position of phenylalanine 23 was synthesized on a cellulose membrane matrix. $hIAPP_{1-37}$ was fused to the C-terminus of maltose binding protein (MBP) and incubated with the peptide array membrane for analysis of its recognition of the bound peptides. The level of interaction was detected using an anti-MBP antibody. The letters denote the residue, in the one-letter code, substituted for phenylalanine 23 at each spot: (top) incubation of the membrane with the MBP−IAPP fusion protein and (bottom) incubation of the membrane with MBP as a control.

effects of substitution of this aromatic moiety on the molecular recognition process and inhibition of fibril formation.

Molecular Recognition of $hIAPP_{20-29}$ Peptide Analogues by $hIAPP_{1-37}$. To systematically explore the molecular determinants that facilitate recognition between hIAPP and its amyloidogenic core ($hIAPP_{20-29}$), a nonbiased peptide array screen was used. We probed the capacity of hIAPP fused to the C-terminus of the maltose binding protein (MBP) to interact with an array of 19 membrane-bound decamer peptides (SNNXGAILSS, where X represents position 23), in which the phenylalanine 23 position was altered with any of the natural amino acids except cysteine (Figure 1). The decamers system was used as it was previously demonstrated to allow detection of high-affinity binding between hIAPP and peptide fragments (*30*). Thus, it allowed sensitive analysis of molecular determinants that mediate this interaction.

Binding to peptides that contained the aromatic tryptophan, phenylalanine, and tyrosine residues was clearly observed (Figure 1). Binding was also observed with the positively charged analogues. In marked contrast, no binding was observed with any of the four hydrophobic substitutions at this position (leucine, isoleucine, valine, and alanine). As a control, an identical peptide array membrane was incubated with MBP alone under the same experimental conditions (Figure 1). In clear contrast to the MBP−IAPP binding assay, no significant binding could be observed with the MBP incubation.

Moreover, when we studied the amyloid forming potential of peptide analogues containing substitutions with all four naturally occurring hydrophobic amino acids using the aggregation assay, all the hydrophobic analogue peptides revealed a very low aggregation capacity, as reflected by solution turbidity (Figure 2A). To determine whether aggregation of the hydrophobic analogues occurs with extremely slow kinetics, solutions of the peptides under the same experimental conditions were incubated for 1 week, exhibiting relatively low turbidity for all hydrophobic analogues (Figure 2B). Ultrastructural visualization of the analogues using TEM also revealed that well-ordered fibrils were only observed with the $hIAPP_{22-29}$ peptide NFGAILSS (Figure 2C). Considerably less ordered aggregates could be detected with the leucine analogue and to a much lower extent with the alanine analogue (NLGAILSS and NAGAILSS, respectively). However, these structures were significantly less abundant, and did not have the typical amyloid structure. No ordered structures were observed with the isoleucine and valine hydrophobic analogues (NIGAILSS and NVGAILSS, respectively).

Inhibition of hIAPP Fibril Formation with the Tyrosine Analogue Peptide. The fact that the tyrosine NYGAILSS analogue could interact with the hIAPP protein (Figure 1), but did not form amyloid fibers itself (*21*), led us to the notion that this peptide may inhibit amyloid formation. This peptide was particularly attractive, since despite the completely different amyloidogenic potential, it is almost chemically identical to the highly amyloidogenic native peptide. Thus, the peptide may preserve all the molecular recognition parameters on one hand and may prevent further amyloid assembly on the other.

To examine this idea, we studied the ability of the tyrosine peptide analogue (NYGAILSS) to inhibit amyloid formation by full-length $hIAPP_{1-37}$. A thioflavin T (ThT) fluorescence assay confirmed the inhibitory effect of this peptide (Figure 3A). After a lag phase of approximately 20 h, $hIAPP_{1-37}$ alone exhibited a logarithmic increase in fluorescence, while addition of NYGAILSS had a strong inhibitory effect, showing a reduced linear increase in fluorescence levels (Figure 3A). The inhibition level of the tyrosine peptide analogue was significantly higher compared to that of the β-breaker peptide methodology (*11*). Even after incubation for 1 week, the NYGAILSS peptide displays a low level of fluorescence relative to the recognition motif peptide conjugated to the proline β-sheet breaker (NFGAILPP) (Figure 3B). Circular dichroism analysis revealed that $hIAPP_{1-37}$ alone underwent a transition from a random coil conformation to a β-sheet conformation (Figure 3C). An initial structural transition to a β-sheet structure was evident after 6 h, reaching a maximum after 26 h (Figure 3C). However, when the NYGAILSS peptide was added to $hIAPP_{1-37}$, no transition to a β-sheet conformation was evident in the first 24 h, and an initial transition was observed after only 4 days (Figure 3D). Although nonquantitative, the ultrastructural analysis using TEM was also consistent with the spectroscopic data. While $hIAPP_{1-37}$ alone formed distinct characteristic fibrils within 30 h, and aggregated mature fibrils within 48 h (panels A and B of Figure 4, respectively), addition of NYGAILSS had a significant inhibitory effect. The amount of fibrillar structures on the TEM grid was much lower, and less distinct characteristic amyloid morphology was evident after 30 h (Figure 4C). Some fibrils that resembled an earlier stage (at 30 h) were evident after 48 h (Figure 4D). The observation of a small amount of fibrils using TEM reflects the high sensitivity of the microscopy analysis. Although this method is not quantitative, it allows the detection of single molecular assemblies that obviously cannot be detected by bulk methods. Addition of the NFGAILSS peptide to hIAPP under the same conditions accelerated fibril formation, as previously reported by Scrocchi *et al.* (*32*) for the NFGAIL hexapeptide, and mature fibrils were clearly observed on the TEM grid after 30 h (Figure 4E). Addition of the NRGAILSS peptide, which exhibited some level of interaction with hIAPP in the molecular recognition assay, had no inhibitory effect, and fibrils, of typical wild-type morphology, were observed after 30 h (Figure 4F).

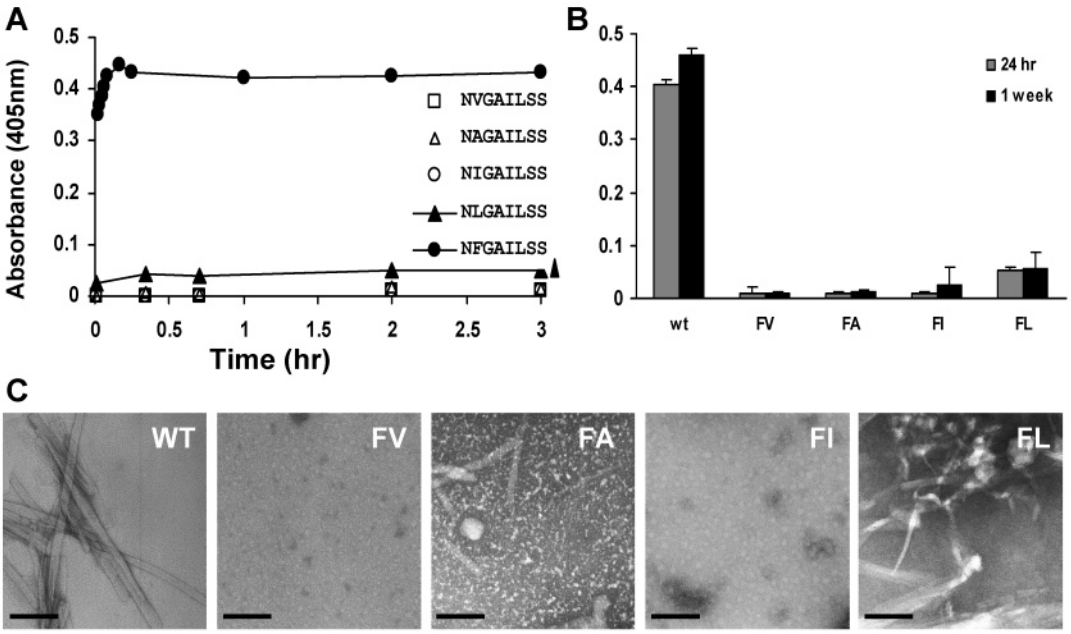

FIGURE 2: Aggregation of the $hIAPP_{22-29}$ peptide and hydrophobic analogues. Aggregation was initiated by diluting a peptide stock solution in Tris-HCl buffer (pH 6.5) to a final peptide concentration of 1 mM and 4% DMSO. Hydrophobic analogues included replacement of phenylalanine 23 with valine, alanine, isoleucine, or leucine. (A) Time-dependent turbidity of hydrophobic analogues of the $hIAPP_{22-29}$ peptide at 405 nm. (B) End-point turbidity of the same peptides after incubation for 1 week. (C) TEM micrographs of the aggregated peptides after incubation for 48 h. Samples were negatively stained with 2% uranyl acetate. The letters denote the amino acid residue, in the one-letter code, substituted for phenylalnine 23 in the NFGAILSS peptide. The bar represents 100 nm.

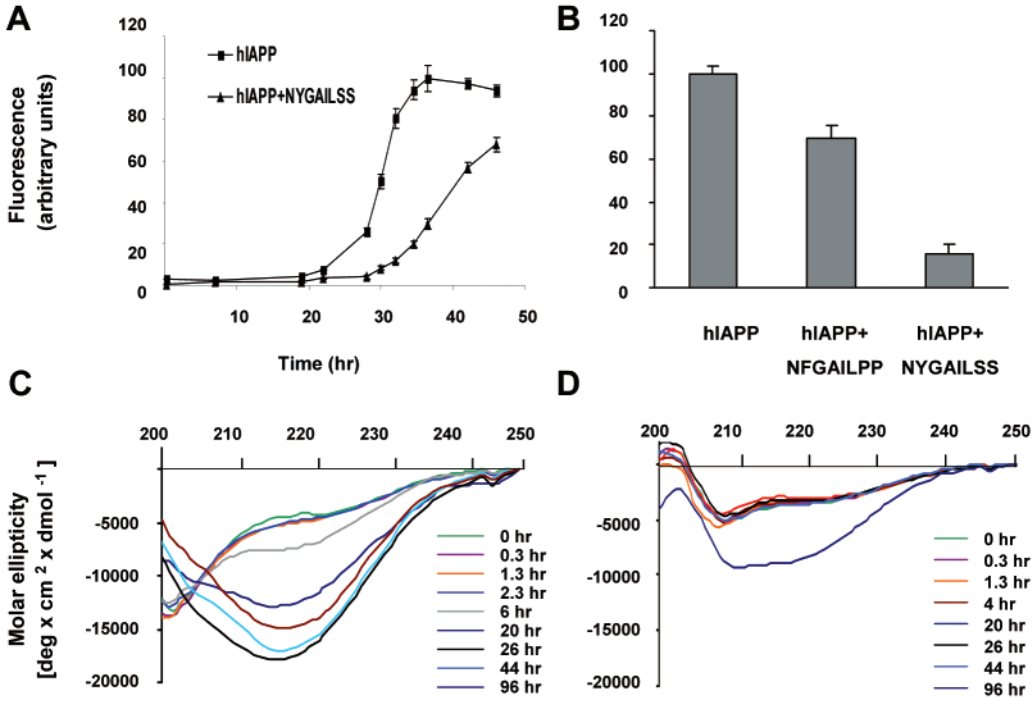

FIGURE 3: Inhibition of $hIAPP_{1-37}$ fibril formation by the NYGAILSS peptide. Human $IAPP_{1-37}$ was dissolved in HFIP and diluted in sodium acetate buffer (pH 6.5) to a final concentration of 4 μM and 1% HFIP, and the nonsoluble peptide was separated by centrifugation. (A) Thioflavin T fluorescence values of $hIAPP_{1-37}$ and 40 μM NYGAILSS peptide. (B) End point fluorescence values after incubation of $hIAPP_{1-37}$ for 5 days in the absence or presence of a β-sheet breaker NFGAILPP and tyrosine analogue NYGAILSS peptide. (C) Circular dichroism of 4 μM $hIAPP_{1-37}$ shows the transition from a random coil conformation to a β-sheet conformation within 6 h. (D) Circular dichroism of 4 μM $hIAPP_{1-37}$ with 40 μM NYGAILSS, showing an inhibited transition to a β-sheet. The spectra of the inhibitor in buffer (see the Supporting Information) were subtracted from the corresponding final spectra.

Inhibition of hIAPP Fibril Formation with a Small Polyphenol Molecule. Our mechanistic insights into amyloid formation, the reported data on the suppressive effect of aromatic compounds (*14*−*17*), and the results given above on the inhibitory effect of tyrosine analogue led us to search for nontoxic, low-molecular weight aromatic compounds that could inhibit hIAPP amyloid formation. Due to the apparent mode of interaction between phenol and benzene moieties in the peptide inhibitor system, we launched a comprehensive search for inhibitory phenolic molecules using a series of

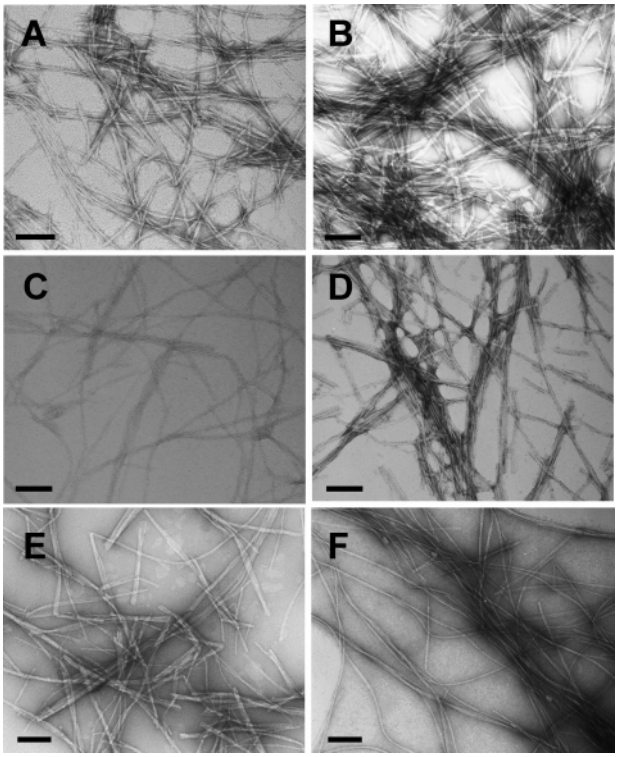

FIGURE 4: Ultrastructural morphology of hIAPP fibrils and peptide inhibition effect. TEM micrographs of $hIAPP_{1-37}$ samples from the inhibition assay in the initial phase of fibril formation (30 h) and after 48 h. (A and B) hIAPP without inhibitors after 30 and 48 h, respectively. (C and D) hIAPP with NYGAILSS peptide after 30 and 48 h, respectively. (E) hIAPP with NFGAILSS peptide after 30 h. (F) hIAPP with NRGAILSS peptide after 30 h. Samples were negatively stained with 2% uranyl acetate. The bar represents 100 nm.

synthetic and natural polyphenol compounds. Phenol red, a nontoxic aromatic compound, was found to be an effective compound for amyloid inhibition.

Addition of phenol red to $hIAPP_{1-37}$ had a strong inhibitory effect on fibril formation that exceeded that of the tyrosine peptide analogue. The ThT fluorescence assay for variable concentrations of phenol red demonstrated concentration-dependent inhibition. Higher phenol red concentrations (more than 4-fold greater than that of hIAPP) have shown constant low fluorescence levels for at least 48 h, while hIAPP had a logarithmic increase in fluorescence levels after 24 h (Figure 5A). Even after incubation for 1 week, the concentration-dependent inhibition was similar (Figure 5B), and an inhibition level of ~90% was achieved for a phenol red concentration of ≥ 20 μM. CD results showed that addition of phenol red to hIAPP caused evident inhibition of the transition from a random coil conformation to a β-sheet conformation for at least 46 h, and a very slow transition after 96 h (Figure 5C). Electron microscopy showed that in contrast to the distinct dense morphology of the fibrils formed by the peptide alone (Figure 5E, 30 h), no fibrils were visualized after 30 h when phenol red was included (Figure 5F). Only after incubation for 48 h were some fibrils observed, and they were much less abundant on the TEM grid than the IAPP control (Figure 5G). However, these fibrils lacked the typical dense morphology as observed with the IAPP control amyloidogenic fibrils (Figures 4A and 5E). Such changes in morphology of the fibrils were observed upon inhibition of fibril formation by the Aβ protein by its pentapeptide fragment (*33*). This pentapeptide currently serves as a lead for the development of Aβ inhibitor drugs. To verify the effect of phenol red inhibition on hIAPP cytotoxicity, a general PC12 cell line was used to measure cytotoxicity in a concentration-dependent manner. Cells were grown in a 96-well plate with or without a gradual concentration of phenol red, and fresh hIAPP was added to the growth medium. After incubation for 24 h, cell viability was measured by MTT reduction assay, and calculated by substitution of the absorbance of IAPP samples with non-IAPP controls containing the same phenol red concentrations. The MTT cell viability assay showed a concentration-dependent rescue of the cells (Figure 5D).

Inhibition of the IAPP Cytotoxic Effect on β Cells. We studied the ability of phenol red to modulate the cytotoxicity of hIAPP amyloid assemblies to pancreatic β-cells in culture. We used a highly differentiated murine β-cell line (βTC-tet) (*31*) with a normal insulin secretory response to glucose. Cells were grown with or without phenol red, and fresh hIAPP was added to the growth medium. An MTT cell viability assay clearly revealed that the presence of phenol red in the medium protected β-cells from the cytotoxic effect of hIAPP assemblies and increased cell viability from 50 to 80% ($P < 0.05$) (Figure 6A). Scanning electron microscopy (SEM) analysis of β-cells that were grown in the presence of hIAPP showed an extensive membrane blebbing (Figure 6B), as previously reported for hIAPP cytotoxicity (*34*), and a collapse of typical cellular morphology in the vast majority of cells (Figure 6D). On the other hand, practically no significant difference could be observed between untreated cells (Figure 6H) and cells grown in the presence of hIAPP and phenol red (Figure 6F). In both cases, most of the cells maintained normal morphology. No blebbing was visible, and membrane extensions of microspikes and lamellipodia were present. Furthermore, upon low-magnification SEM examination, normal arrays of β-cells could be observed with the phenol red-protected cells and control cells (panels E and G of Figure 6, respectively). In marked contrast, only isolated and morphologically altered cells could be observed upon IAPP incubation with no phenol red protection (Figure 6C).

To study the ability of the NYGAILSS peptide to inhibit hIAPP cytotoxicity, we have added 40 μM NYGAILSS peptide to the growth medium. Apparently, this concentration of NYGAILSS was cytotoxic to βTC-tet cells and decreased β-cell viability to 20% of control, without hIAPP addition (Figure 6A). Therefore, NYGAILSS could not be used as a cytotoxicity inhibitor.

DISCUSSION

Although the formation of amyloid fibrils is associated with major human diseases, its exact mechanism of formation is not fully understood. The genuine understanding of the mechanism that leads to the formation of amyloid fibrils and its inhibition is therefore highly clinically important. The core amyloidogenic module of the type 2 diabetes-related hIAPP serves as an excellent model system for studying the molecular mechanism of amyloid fibril formation (*18*−*20*). This is due to the fact that such a small fragment contains all the structural information needed to mediate the self-

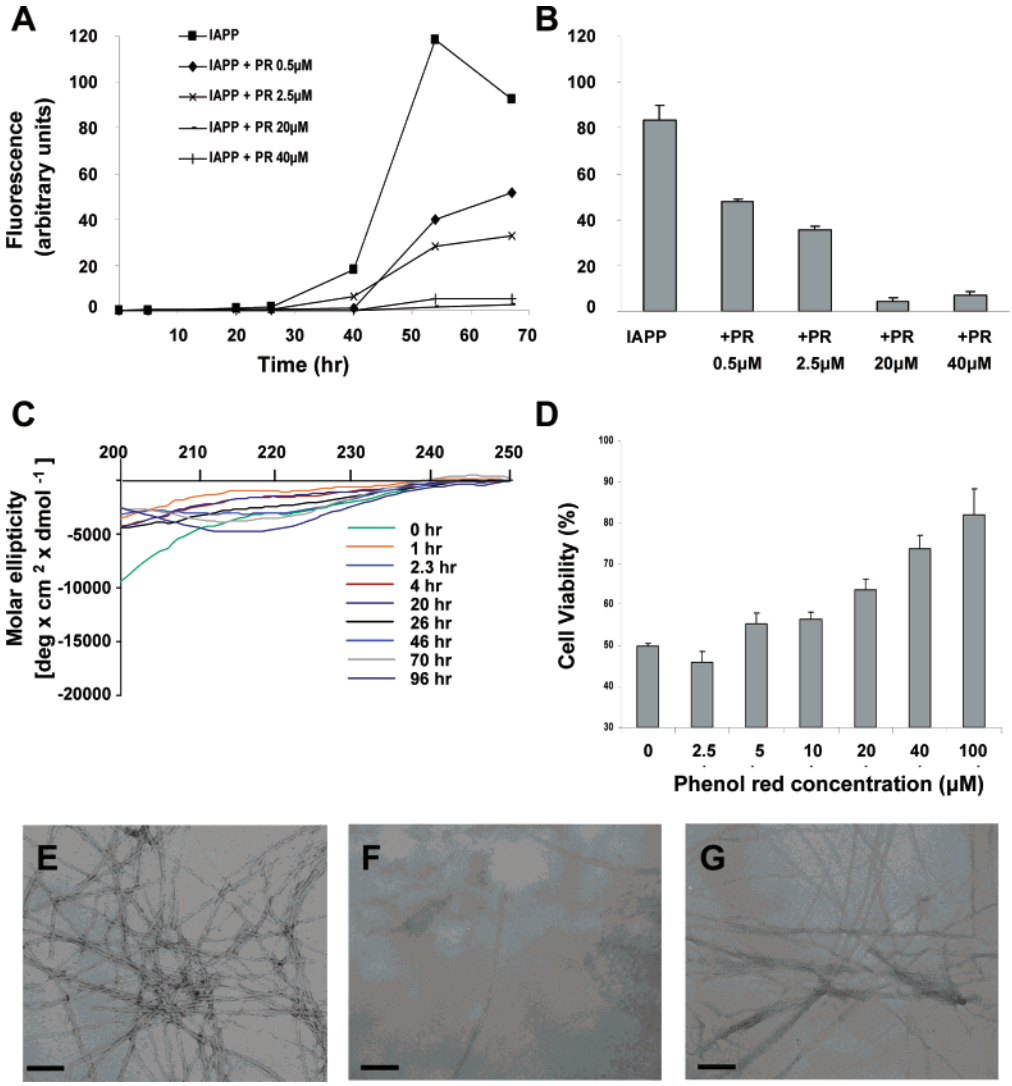

FIGURE 5: Inhibition of $hIAPP_{1-37}$ fibril formation and cytotoxicity by the phenol red molecule. Human IAPP was dissolved in HFIP and diluted to a final concentration of 5 μM with a gradual concentration of a phenol red molecule as an inhibitor. (A) Thioflavin T fluorescence kinetic values of $hIAPP_{1-37}$ and gradual concentration of phenol red result in a dose-dependent inhibition. (B) End point fluorescence of the same samples after incubation for 5 days. Values are means ± the standard deviation ($n = 3$). (C) Circular dichroism spectra of 4 μM $hIAPP_{1-37}$ with 40 μM phenol red show an inhibited transition from a random coil conformation to a β-sheet. Only after 70−96 h there is some transition to a β-sheet conformation. The spectra of phenol red in buffer (see the Supporting Information) were subtracted from the corresponding final spectra. (D) Cytotoxicity assay of $hIAPP_{1-37}$ and gradual concentrations of phenol red toward PC12 cells. Values are means ± the standard deviation ($n = 4$). (E−G) Ultrastructural morphology using TEM of 4 μM $hIAPP_{1-37}$ and 40 μM phenol red from the fluorescence inhibition assay. $hIAPP_{1-37}$ without the inhibitor after incubation for 30 h shows distinct characteristic dense fiber formation (E), while in the presence of phenol red, no fibrils were visualized after 30 h when phenol red was included (F). After incubation for 48 h, some fibrils that were much less abundant on the TEM grid were observed (G).

assembly and molecular recognition processes that lead to the formation of amyloid structures. Here, we demonstrate that substitution of the key phenylalanine 23 residue with the other natural aromatic amino acids still enabled the molecular recognition between the full-length $IAPP_{1-37}$ and its core module, SNNFGAILSS (Figure 1). On the other hand, substitution of phenylalanine 23 with any of the other natural hydrophobic amino acids completely impeded the molecular recognition process (Figure 1). Moreover, substitution of the phenylalanine residue with other hydrophobic amino acids also completely prevented aggregation of the peptides (Figure 2).

Therefore, the effect of these substitutions is unlikely to merely reflect a change in hydrophobicity. In addition, this effect does not seem to reflect the ability to form β-sheet structures, the common structural component of fibrils, as isoleucine and valine are considered to be more efficient β-sheet formers than phenylalanine. Therefore, we suggest that aromatic interactions are an important factor in the process that leads to amyloid fibril formation. This notion is in agreement with recent studies on *de novo*-designed peptides that suggested that hydrophobic interactions could not simply account for the formation of fibrils and that specific interactions are crucial in the stabilization of fibrillar aggregates (*35*).

Interestingly, the tyrosine peptide analogue, NYGAILSS, demonstrated a clear recognition of hIAPP in the peptide array assay (Figure 1), but had no amyloidogenic activity (*21*). We speculated that the difference in the molecular nature of tyrosine pair interactions, as compared to phenylalanine pairs, accounts for the difference in the amyloidogenic potential. It was recently demonstrated, using

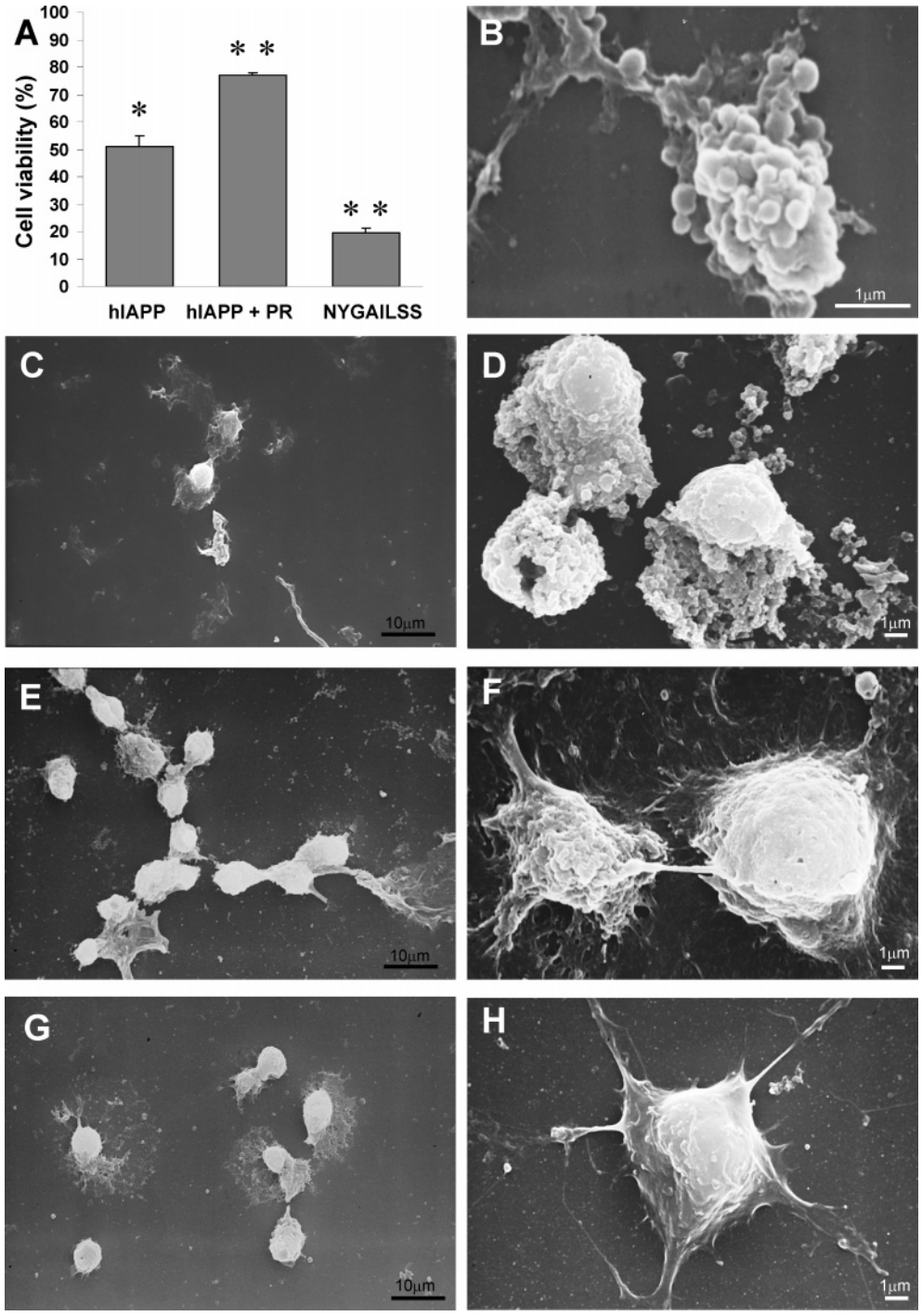

FIGURE 6: Inhibition of hIAPP cytotoxicity toward β-cells. βTC-tet rodent β-cells (*31*) were incubated for 24 h with 4 μM hIAPP$_{1-37}$ in serum free DMEM with or without phenol red, and viability was measured using the MTT reduction assay. (A) β-Cell viability compared to that of cells incubated in the absence of hIAPP, in medium with or without phenol red, and the NYGAILSS control without IAPP. Values are means $\pm$ the standard deviation ($n = 4$). $p = 0.03$ (one asterisk), and $p < 0.005$ (two asterisks). SEM analysis of β-cells grown on microscope coverslips under the same conditions. (B−D) β-Cells after addition of hIAPP alone display membrane blebbing and collapse. (E and F) β-Cells after addition of hIAPP in the presence of 40 μM phenol red in the growth medium. (G and H) Control β-cells that were incubated under the same conditions without addition of hIAPP.

molecular dynamics simulations (*36*), that phenylalanine pairs are preferentially arranged in a parallel displaced geometry that is consistent with aromatic stacking. The simulation revealed one predominant (91% of the population) phenylalanine−phenylalanine energetically favored stacked state, with 4.5 Å distance between the two ring centroids, which is consistent with β-sheet stacking. On the other hand, the tyrosine−tyrosine pair had eight different states of minimum energy with no predominant structure. The most common structure that represented 26.1% of the population had a T-shape orientation with a distance of 5.9 Å (*36*).

The concept of differential geometry of aromatic interactions led us to test the ability of the NYGAILSS peptide to serve as an inhibitor of amyloid fibril formation by IAPP. The molecular dynamics studies of the heteroaromatic phenylalanine−tyrosine pair (*36*) revealed that the most

common phenylalanine−tyrosine geometry (64.7%) has an oblique orientation with an angle of 31.7° between the two normals to the ring. The stacked and T-shape geometries were much less common (31.4 and 3.9%, respectively). Indeed, the NYGAILSS peptide demonstrated a very significant inhibitory activity as reveled independently by ThT fluorescence (Figure 3), circular dichroism secondary structure analysis (Figure 3), and electron microscopy (Figure 4). On the other hand, the NFGAILSS peptide accelerated fibril formation, as previously reported for the NFGAIL peptide (*32*). The NRGAILSS peptide, which had some level of molecular recognition of IAPP, had no inhibition effect. We assume that the NYGAILSS peptide's ability to interact with IAPP (Figure 1), yet in a geometry that is inconsistent with amyloid formation, may account for such a significant inhibitory effect.

Another approach to amyloid fibril inhibition is the use of low-molecular weight inhibitors. The concept of unique geometrical constraints of heteroaromatic interactions led us to search for various polyphenolic compounds. Among the compounds, phenol red was found to be a remarkable inhibitor of IAPP fibril formation *in vitro* (Figure 5). Moreover, pheonl red demonstrated a very efficient protection of pancreatic β-cells from the cytotoxic effect of IAPP (Figure 6). This result is quite intriguing as phenol red is a simple, safe, nontoxic, and noncarcinogenic compound that has been used for many years in tissue culture with no adverse effect. The concept of inhibition of amyloid fibril formation by polyphenols was independently demonstrated by the efficient *in vitro* inhibition of the Alzheimer's β-amyloid polypeptide by wine polyphenols (*37*). However, a clear mechanism of inhibition was not suggested (*37*).

Taken together, our current study provides further experimental support for the role of aromatic interactions in the self-assembly of IAPP amyloid fibrils, using a comprehensive nonbiased analysis. It also demonstrates the ability of a short tyrosine-modified peptide and a small polyphenol molecule to effectively inhibit the formation of amyloid fibrils by hIAPP. These results, taken together with the demonstration of amyloid formation inhibition by polycyclic molecules (*14*, *37*) and the formation of amyloid fibrils by short aromatic peptides (*20*−*25*, *38*), further imply the use of aromatic recognition motifs as targets for molecular design. We assume that the inhibitory aromatic compounds compete with the polypeptide monomers for interaction with the growing fibrils. Irreversible or improved interaction by the inhibitor should result in an efficient halt of the fibrillization process.

ACKNOWLEDGMENT

We thank Y. Delarea from the TAU electron microscopy unit for help with TEM and SEM experiments and M. Bar-Chen and K. Hollander for help with tissue culture. We thank members of the Gazit laboratory for helpful discussions.

SUPPORTING INFORMATION AVAILABLE

CD spectra of NYGAILSS and phenol red inhibitors. This material is available free of charge via the Internet at http://pubs.acs.org.

REFERENCES

1. Harper, J. D., and Lansbury, P. T., Jr. (1997) Models of amyloid seeding in Alzheimer's disease and scrapie: mechanistic truths and physiological consequences of the time-dependent solubility of amyloid proteins, *Annu. Rev. Biochem. 66*, 385−407.
2. Dobson, C. M. (2003) Protein folding and misfolding, *Nature 426*, 884−890.
3. Johnson, K. H., O'Brien, T. D., Betsholtz, C., and Westermark, P. (1989) Islet amyloid, islet-amyloid polypeptide, and diabetes mellitus, *N. Engl. J. Med. 321*, 513−518.
4. Kapurniotu, A. (2001) Amyloidogenicity and cytotoxicity of islet amyloid polypeptide, *Biopolymers 60*, 438−459.
5. Höppener, J. W., Ahrén, B., and Lips, C. J. (2000) Islet amyloid and type 2 diabetes mellitus, *N. Engl. J. Med. 343*, 411−419.
6. Anguiano, M., Nowak, R. J., and Lansbury, P. T., Jr. (2002) Protofibrillar islet amyloid polypeptide permeabilizes synthetic vesicles by a pore-like mechanism that may be relevant to type II diabetes, *Biochemistry 41*, 11338−11343.
7. Porat, Y., Kolusheva, S., Jelinek, R., and Gazit, E. (2003) The human islet amyloid polypeptide forms transient membrane-active prefibrillar assemblies, *Biochemistry 42*, 10971−10977.
8. Bucciantini, M., Giannoni, E., Chiti, F., Baroni, F., Formigli, L., Zurdo, J., Taddei, N., Ramponi, G., Dobson, C. M., and Stefani, M. (2002) Inherent toxicity of aggregates implies a common mechanism for protein misfolding diseases, *Nature 416*, 507−511.
9. Sacchettini, J. C., and Kelly, J. W. (2002) Therapeutic strategies for human amyloid diseases, *Nat. Rev. Drug Discovery 1*, 267−275.
10. Cohen, F. E., and Kelly, J. W. (2003) Therapeutic approaches to protein-misfolding diseases, *Nature 426*, 905−909.
11. Soto, C., Sigurdsson, E. M., Morelli, L., Kumar, R. A., Castaño, E. M., and Frangione, B. (1998) β-Sheet breaker peptides inhibit fibrillogenesis in a rat brain model of amyloidosis: implications for Alzheimer's therapy, *Nat. Med. 4*, 822−826.
12. Findeis, M. A., Musso, G. M., Arico-Muendel, C. C., Benjamin, H. W., Hundal, A. M., Lee, J. J., Chin, J., Kelley, M., Wakefield, J., Hayward, N. J., and Molineaux, S. M. (1999) Modified-peptide inhibitors of amyloid β-peptide polymerization, *Biochemistry 38*, 6791−6800.
13. Kayed, R., Head, E., Thompson, J. L., McIntire, T. M., Milton, S. C., Cotman, C. W., and Glabe, C. G. (2003) Common structure of soluble amyloid oligomers implies common mechanism of pathogenesis, *Science 300*, 486−489.
14. Aitken, J. F., Loomes, K. M., Konarkowska, B., and Cooper, G. J. (2003) Suppression by polycyclic compounds of the conversion of human amylin into insoluble amyloid, *Biochem. J. 374*, 779−784.
15. Kuner, P., Bohrmann, B., Tjernberg, L. O., Näslund, J., Huber, G., Celenk, S., Grüninger-Leitch, F., Richards, J. G., Jakob-Rœtne, R., Kemp, J. A., and Nordstedt, C. (2000) Controlling polymerization of β-amyloid and prion-derived peptides with synthetic small molecule ligands, *J. Biol. Chem. 275*, 1673−1678.
16. Harroun, T. A., Bradshaw, J. P., and Ashley, R. H. (2001) Inhibitors can arrest the membrane activity of human islet amyloid polypeptide independently of amyloid formation, *FEBS Lett. 507*, 200−204.
17. Lashuel, H. A., Hartley, D. M., Balakhaneh, D., Aggarwal, A., Teichberg, S., and Callaway, D. J. (2002) New class of inhibitors of amyloid-β fibril formation. Implications for the mechanism of pathogenesis in Alzheimer's disease, *J. Biol. Chem. 277*, 42881−42890.
18. Westermark, P., Engström, U., Johnson, K. H., Westermark, G. T., and Betsholtz, C. (1990) Islet amyloid polypeptide: pinpointing amino acid residues linked to amyloid fibril formation, *Proc. Natl. Acad. Sci. U.S.A. 87*, 5036−5040.
19. Tenidis, K., Waldner, M., Bernhagen, J., Fischle, W., Bergmann, M., Weber, M., Merkle, M. L., Voelter, W., Brunner, H., and Kapurniotu, A. (2000) Identification of a penta- and hexapeptide of islet amyloid polypeptide (IAPP) with amyloidogenic and cytotoxic properties, *J. Mol. Biol. 295*, 1055−1071.
20. Azriel, R., and Gazit, E. (2001) Analysis of the minimal amyloid-forming fragment of the islet amyloid polypeptide. An experimental support for the key role of the phenylalanine residue in amyloid formation, *J. Biol. Chem. 276*, 34156−34161.
21. Porat, Y., Stepensky, A., Ding, F. X., Naider, F., and Gazit, E. (2003) Completely different amyloidogenic potential of nearly identical peptide fragments, *Biopolymers 69*, 161−164.
22. Reches, M., Porat, Y., and Gazit, E. (2002) Amyloid fibril formation by pentapeptide and tetrapeptide fragments of human calcitonin, *J. Biol. Chem. 277*, 35475−35480.

23. Jones, S., Manning, J., Kad, N. M., and Radford, S. E. (2003) Amyloid-forming peptides from β2-microglobulin: Insights into the mechanism of fibril formation *in vitro*, *J. Mol. Biol. 325*, 249−257.
24. Gazit, E. (2002) A possible role for π-stacking in the self-assembly of amyloid fibrils, *FASEB J. 16*, 77−83.
25. Aggeli, A., Bell, M., Boden, N., Keen, J. N., Knowles, P. F., McLeish, T. C., Pitkeathly, M., and Radford, S. E. (1997) Responsive gels formed by the spontaneous self-assembly of peptides into polymeric β-sheet tapes, *Nature 386*, 259−262.
26. Claessens, C. G., and Stoddart, J. F. (1997) $\pi-\pi$ interactions in self-assembly, *J. Phys. Org. Chem. 10*, 254−272.
27. Burley, S. K., and Petsko, G. A. (1985) Aromatic−aromatic interaction: a mechanism of protein structure stabilization, *Science 229*, 23−28.
28. Hunter, C. A. (1993) Arene-arene interactions: electrostatic or charge transfer, *Angew. Chem., Int. Ed. Engl. 32*, 1584−1586.
29. Reches, M., and Gazit, E. (2003) Casting metal nanowires within discrete self-assembled peptide nanotubes, *Science 300*, 625−627.
30. Mazor, Y., Gilead, S., Benhar, I., and Gazit, E. (2002) Identification and characterization of a novel molecular-recognition and self-assembly domain within the islet amyloid polypeptide, *J. Mol. Biol. 322*, 1013−1024.
31. Fleischer, N., Chen, C., Surana, M., Leiser, M., Rossetti, L., Pralong, W., and Efrat, S. (1998) Functional analysis of a conditionally transformed pancreatic β-cell line, *Diabetes 47*, 1419−1425.
32. Scrocchi, L. A., Chen, Y., Waschuk, S., Wang, F., Cheung, S., Darabie, A. A., McLaurin, J., and Fraser, P. E. (2002) Design of peptide-based inhibitors of human islet amyloid polypeptide fibrillogenesis, *J. Mol. Biol. 318*, 697−706.
33. Tjernberg, L. O., Näslund, J., Lindqvist, F., Iohansson, J., Karlström, A. R., Thyberg, J., Terenius, L., and Nordstedt, C. (1996) Arrest of β-amyloid fibril formation by a pentapeptide ligand, *J. Biol. Chem. 271*, 8545−8548.
34. Saafi, E. L., Konarkowska, B., Zhang, S., Kistler, J., and Cooper, G. J. (2001) Ultrastructural evidence that apoptosis is the mechanism by which human amylin evokes death in RINm5F pancreatic islet β-cells, *Cell Biol. Int. 25*, 339−350.
35. López de la Paz, M., Goldie, K., Zurdo, J., Lacroix, E., Dobson, C. M., Hoenger, A., and Serrano, L. (2002) De novo designed peptide-based amyloid fibrils, *Proc. Natl. Acad. Sci. U.S.A. 99*, 16052−16057.
36. Chelli, R., Gervasio, F. L., Procacci, P., and Schettino, V. (2002) Stacking and T-shape competition in aromatic−aromatic amino acid interactions, *J. Am. Chem. Soc. 124*, 6133−6143.
37. Ono, K., Yoshiike, Y., Takashima, A., Hasegawa, K., Naiki, H., and Masahito, Y. (2003) Potent anti-amyloidogenic and fibril-destabilizing effects of polyphenols in vitro: implications for the prevention and therapeutics of Alzheimer's disease, *J. Neurochem. 87*, 172−181.
38. Reches, M., and Gazit, E. (2004) Amyloidogenic hexapeptide fragment of medin: Implications for the stacking model of fibrillization, *Amyloid 11*, 81−89.

BI048582A